Quantum metrology with imperfect states and detectors

Animesh Datta,[1,*] Lijian Zhang,[1] Nicholas Thomas-Peter,[1] Uwe Dorner,[2,1] Brian J. Smith,[1] and Ian A. Walmsley[1]
[1]*Clarendon Laboratory, Department of Physics, University of Oxford, OX1 3PU, United Kingdom*
[2]*Centre for Quantum Technologies, National University of Singapore, 3 Science Drive 2, 117543 Singapore, Singapore*
(Received 6 December 2010; published 24 June 2011)

Quantum enhancements of precision in metrology can be compromised by system imperfections. These may be mitigated by appropriate optimization of the input state to render it robust, at the expense of making the state difficult to prepare. In this paper, we identify the major sources of imperfection of an optical sensor: input state preparation inefficiency, sensor losses, and detector inefficiency. The second of these has received much attention; we show that it is the least damaging to surpassing the standard quantum limit in a optical interferometric sensor. Further, we show that photonic states that can be prepared in the laboratory using feasible resources allow a measurement strategy using photon-number-resolving detectors that not only attain the Heisenberg limit for phase estimation in the absence of losses, but also deliver close to the maximum possible precision in realistic scenarios including losses and inefficiencies. In particular, we give bounds for the tradeoff between the three sources of imperfection that will allow true quantum-enhanced optical metrology

DOI: 10.1103/PhysRevA.83.063836 PACS number(s): 42.50.St, 03.65.Ta, 42.50.Lc

I. INTRODUCTION

Measurements can be made more precise by using sensor designs based on quantum-mechanical rather than classical physical principles. The proximate cause of this enhanced precision is the reduced measurement noise enabled by quantum entanglement. The realization of these advantages therefore hinges upon the preparation of particular nonclassical states that encode the sensor state parameter in such a manner as to allow its determination with precision beyond the standard quantum limit (SQL) [1]. Given a quantum state, the ultimate limit on the attainable precision is provided by the quantum Cramér-Rao bound (QCRB) via the quantum Fisher information (QFI) [2]. Early theoretical efforts in quantum metrology centered around designing quantum states that saturate this bound.

A paradigm for quantum-enhanced measurement is optical interferometry, in which the phase difference between two field modes is to be estimated. For fixed photon numbers and no losses, quantum states minimizing the QCRB are the so-called $N00N$ states, consisting of a superposition of N photons in one mode and none in the other [3–5]. Unfortunately, $N00N$ states are exponentially more vulnerable to losses than classical states, and quickly lose their capacity for enhanced sensing. More recently, the effects of loss in an interferometer have been considered [6–9]. The optimal states for lossy phase estimation are, not surprisingly, dependent on the exact value of the loss in the interferometer. Consequently, no universal scheme for their preparation is possible.

However, losses in the interferometer are not the only imperfections to be dealt with. Preparation of the input state may be inefficient, delivering only an approximate version of the desired probe state. Also, the detectors may not be efficient and may not implement the requisite measurement strategy. In this paper, we encompass imperfect input state preparation and sensor output measurement into our analysis. We show, surprisingly, that such imperfections are more detrimental to sensor performance than internal losses. However, we are able to identify a class of states that are close to optimally robust against such imperfections, and yet are feasibly constructed in the laboratory. This gives hope that the challenges of a palpably nonclassical sensor may be operated in realistic conditions. Since any implementation of quantum metrology will inevitably have all three imperfections, our results identify the range of imperfections and losses under which we can still demonstrate an objective advantage over classical phase estimation. They also pinpoint exactly the tradeoffs and bottlenecks in the path of demonstrating quantum-enhanced metrology under realistic conditions. Our paper addresses the fundamental gap between the principle and practice of quantum metrology. Furthermore, our paper illustrates the usefulness of nonmaximally entangled states.

Our scheme, shown in Fig. 1, starts with N photons in each of two modes given by $|\Psi\rangle = |N\rangle|N\rangle$, which can be generated in a heralded manner with nonlinear processes such as parametric down conversion and photon-number-resolving detectors (PNRDs) [10], incident onto a 50:50 beam splitter. The resulting state [see Eq. (1)], which we denote HB(N), was proposed by Holland and Burnett [11], has a photon-number variance quadratic in N, and thus is capable of attaining the Heisenberg limit for phase estimation [2]. They are more feasible in terms of laboratory resources than $N00N$ and optimal states, yet their performance is not drastically diminished in the presence of losses [12]. Recent work has demonstrated a scalable route to prepare highly pure HB(N) states, relying on production of Fock states without complex linear-optical networks [10]. In contrast, $N00N$ states require not only the generation of N photons, but also a manipulation of these photons by means of a complex linear-optical network [13]. The output of such a network is probabilistic since it relies on a particular detection (or nondetection) event of ancillary photons. This success probability usually decreases exponentially with increasing photon numbers. Schemes that can, in principle, generate $N00N$ states with high success probability require either high nonlinearity [14] or actively controlled cavities [15], which challenge current technology. This decreasing probability of production necessitates post

*animesh.datta@physics.ox.ac.uk

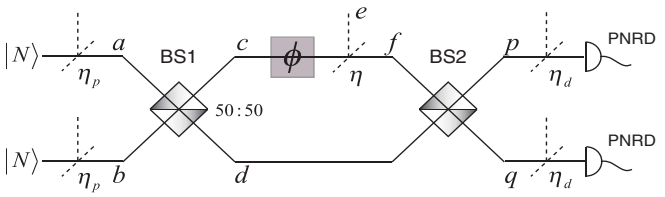

FIG. 1. (Color online) A schematic interferometer involving HB(N) states. BS1 and BS2 are 50/50 beam splitters, ϕ denotes the phase shift of mode c, and PNRD is a photon-number-resolving detector. η is the loss in the interferometer arm, while η_p and η_d are the preparation and detection imperfections. $\eta = \eta_p = \eta_d = 1$ denotes a perfect setup.

selection on the outcomes to exhibit any perceived quantum enhancements.

II. HOLLAND-BURNETT STATES

We show that, for HB(N) states, the QFI for phase estimation can be achieved with PNRDs. Fisher information also allows for an objective, situation-independent, resource-based certificate for our metrology scheme. We begin by calculating the QFI for phase estimation attainable with HB(N) states in an ideal interferometer (Fig. 1). After BS1, $\sqrt{2}a^\dagger \to c^\dagger + d^\dagger, \sqrt{2}b^\dagger \to c^\dagger - d^\dagger$, and the phase shifter $c^\dagger \to e^{i\phi}c^\dagger$,

$$|\Psi\rangle = \sum_{n=0}^{N} A_n |2n, 2N-2n\rangle, \quad A_n = \frac{\sqrt{2n!(2N-2n)!}}{2^N n!(N-n)!} e^{2in\phi}, \tag{1}$$

where ϕ is the parameter to be estimated. The QFI quantifies changes in the initial state as a result of accumulating phase. This gives $d|\Psi\rangle/d\phi \equiv |\Psi_\phi\rangle = \sum_{n=0}^{N} 2nA_n|2n, 2N-2n\rangle$, leading to a QFI of [2]

$$\mathcal{J} = 4(\langle\Psi_\phi|\Psi_\phi\rangle - |\langle\Psi|\Psi_\phi\rangle|^2). \tag{2}$$

Since $\langle\Psi_\phi|\Psi_\phi\rangle = N(3N+1)/2$, and $\langle\Psi|\Psi_\phi\rangle = iN$,

$$\mathcal{J} = 2N(N+1). \tag{3}$$

This quantity, through the QCRB, $\Delta\phi \geqslant 1/\sqrt{\mathcal{J}}$, provides the absolute attainable precision in phase estimation [2] using HB(N) states. The quadratic behavior of the QFI with the number of particles involved shows that we attain the Heisenberg limit. The original suggestion [11] of measuring the number difference in the two modes after BS2 (Fig. 1) contains no information about the phase [16]. A parity measurement Π_N on one of the resulting modes leads to $\langle\Pi_N\rangle = P_N(\cos 2\phi)$, where $P_N(\cdots)$ are Legendre polynomials. This provides a bound commensurate with Eq. (3). Parity measurements are possible on the field mode [19], but require additional resources including a local oscillator reference beam that is well matched to the probe state. Our endeavor here is to introduce a set of measurements that attains this limit, can be built from feasible laboratory resources, and is robust to imperfections such as inefficient detectors.

We show that a beam splitter and PNRDs suffices to saturate the QCRB. Mixing modes f and d on BS2 yields $\sqrt{2}f^\dagger \to p^\dagger + q^\dagger, \sqrt{2}d^\dagger \to p^\dagger - q^\dagger$. Number-resolving measurements $|n\rangle_p|2N-n\rangle_q$ on the two modes yield $p_n = n![P_N^{N-n}(\cos\phi)]^2/(2N-n)!$, where $0 \leqslant n \leqslant N$, and $P_N^l(\cdots)$ are the associated Legendre polynomials. The expression for $N \leqslant n \leqslant 2N$ is obtained by substituting $n \to 2N-n$. A simple yet interesting case is when we *only* make the measurement $|N\rangle_p|N\rangle_q$. The resulting probability function $p_N = [P_N(\cos\phi)]^2$ has the same periodicity as the result of a parity measurement, and the Fisher information for this situation scales exactly as the Heisenberg limit in Eq. (3), just like the parity measurement [17]. Thus, the Heisenberg limit for phase estimation with lossless interferometers can be attained with just one pair of PNRDs. In essence, the external local oscillator necessary for the parity measurement has been replaced by the other arm of the interferometer, greatly simplifying the experimental demands. Photon-number measurements still suffice when there are losses and imperfections, but the required number of measurements rises quadratically with N.

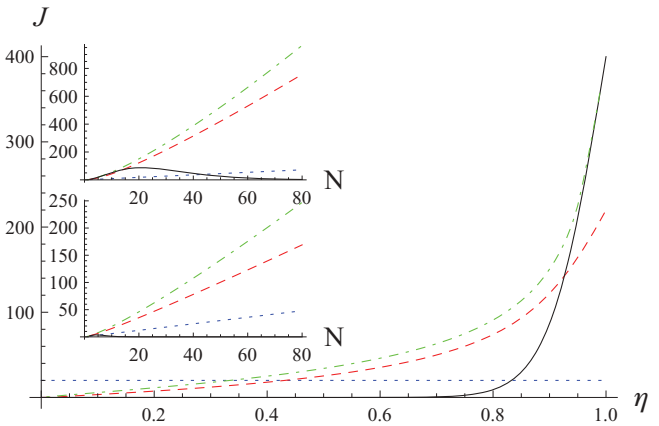

FIG. 2. (Color online) QFI for phase estimation as a function of the transmissivity η for 20 input photons. Blue (dotted line): standard quantum limit. Red (dashed line): HB(10) states. Black (solid line): $N00N$ states. Green (dotted-dashed line): optimal states [7]. Inset: QFI for phase estimation as a function of the photon number N for $\eta = 0.9$ (top) and $\eta = 0.6$ (bottom).

III. LOSSY INTERFEROMETRY

A. Loss in the interferometer

Analysis of the performance of HB(N) states in interferometry in the presence of losses starts with Eq. (1), the loss in a single arm of the interferometer being modeled as $c^\dagger \to \sqrt{\eta}f^\dagger + \sqrt{1-\eta}e^\dagger$, e being an unaccessible environment mode. Most of the loss occurs when the light interacts with the sample for phase accumulation, thus motivating treatment of loss in only one arm. Loss in both arms can be treated similarly, but requires numerical analysis and is beyond the scope of the current work. The subsequent state is

$$|\Psi\rangle = \frac{1}{2^N}\sum_{n=0}^{N}\sum_{m=0}^{2n} C_n B_{n,m}|2n-m\rangle_f|2N-2n\rangle_d|m\rangle_e,$$

where $C_n = 2n!\sqrt{(2N-2n)!}e^{2in\phi}/n!(N-n)!$, $B_{n,m} = \eta^{n-m/2}(1-\eta)^{m/2}/\sqrt{(2n-m)!m!}$, and m is the number of photons lost to the environment. The resulting state obtained

by tracing over mode e is mixed, but its QFI can be calculated as shown in Appendix A. To start with, for $N = 1$,

$$\mathcal{J}_{(N=1)} = 8\frac{\eta^2}{1+\eta^2}, \tag{4}$$

which is the same as that obtained for two-photon $N00N$ states in [7], as expected, since they are identical to HB(1) states. For higher photon numbers, $N00N$ and HB(N) states differ, and HB(N) states are more resilient to losses than the corresponding $N00N$ states with the same number of photons. This is shown in Fig. 2 for $N = 10$, where the QFI for HB(10) exceeds the standard quantum limit for $\eta > 0.45$ and adheres close to that of the optimal states for each value of the loss [7].

B. Imperfect state preparation

We now analyze the performance of HB(N) states in a more realistic situation where their preparation is not ideal. This is more than just with an eye toward experimental demonstration, although that provides part of the motivation. More vital is our desire to address the gap between the theory and practice of quantum metrology. To that end, we will work with the classical Fisher information F obtainable with PNRDs.

We model a scenario where the input state might not necessarily be a twin Fock state $|N\rangle|N\rangle$, as in Fig. 1. Independent of the physical nature of the probes, having exactly an equal number of bosons in two modes is difficult to realize experimentally. In an optical implementation, Fock states can be prepared by heralding [10,18]. In practice, the heralding efficiency is not unity. We can model this situation with ideal Fock state sources followed by a beam splitter of transmissivity η_p in each mode before it is incident on the 50:50 beam splitter. Such a beam splitter leads to $|N\rangle \to \rho \equiv \sum_{n=0}^{N} \binom{N}{n} \eta_p^n (1-\eta_p)^{N-n} |n\rangle\langle n|$. The resulting classical Fisher information, assuming perfect transmission and detection with PNRDs, has a maximum for $\phi = 0$, given by $F_{\eta_p}^{\max} = 2N(N+1)\eta_p^{N+1}$. Interestingly, the minimum is attained for $\phi = \pi/2$, giving $F_{\eta_p}^{\min} = 2N(N+1)\eta_p^{2N}$.

C. Imperfect detection

Finally, we address the scenario where the detectors, PNRDs, are imperfect as well. This situation is modeled by placing beam splitters with transmissivity η_d in front of our PNRDs. We deal with the two simplest cases $N = 1$ and $N = 2$ in order to illustrate key features of the system's performance. These will allow us to identify regimes within which we can unambiguously demonstrate quantum advantage in metrology, once again in a lossy scenario with nonideal sources and detectors. The procedure for obtaining the Fisher information for this scenario explicitly can be found in Appendix B. When there is no loss in the interferometer, $F(\phi = 0) = 2N(N+1)(\eta_p\eta_d)^{N+1}$, illustrating the general principle that the quantum and classical Fisher information are symmetric under exchange of η_p and η_d.

To judge the performance of the HB(k) state in providing genuine quantum advantage in phase estimation, we need to surpass the corresponding standard quantum limit, given by $F^{\mathrm{SQL}} = 2k\eta\eta_d$. This is the standard quantum limit for a classical experiment performed on an apparatus identical to the quantum one, assuming that the classical (coherent) state can be prepared with certainty. The figure of merit for a quantum advantage is the ratio

$$\eth_k(\eta_p,\eta,\eta_d) = \frac{F_{(N=k)}}{F^{\mathrm{SQL}}} \geqslant 1. \tag{5}$$

We begin with HB(1), in which case

$$\eth_1(\eta_p,\eta,\eta_d) = \frac{4\eta_p^2\eta_d\eta}{1+\eta^2} > 1. \tag{6}$$

An expression such as this is very beneficial as it demonstrates the tradeoffs involved in state preparation, interferometer construction, and detection imperfection, which allows experimentalists to direct their efforts appropriately. For instance, if $\eta_d < 0.5$, its is impossible to beat the standard quantum limit with HB(1) states, thereby rendering moot any discussion about the nature of the source and the interferometer. The asymmetry between preparation and detection imperfections in the final reckoning is due to the fact that the state attaining the SQL, a coherent state, can be produced with unit efficiency.

The quantum advantage for HB(2) is addressed by $\eth_2(\eta_p,\eta,\eta_d) = F_{(N=2)}/4\eta\eta_d$, where the right-hand side is maximized over ϕ. To get an idea of the requirements for an experiment, we find numerically that 0.687, 0.135, and 0.547 are the minimum values of η_p, η, and η_d, respectively, required to beat the SQL when the other two are unity. The complete region where $\eth_2(\eta_p,\eta,\eta_d) \geqslant 1$ is depicted in Fig. 3. In general, higher photon number states are more resilient to losses in the interferometer but they also put stricter demands

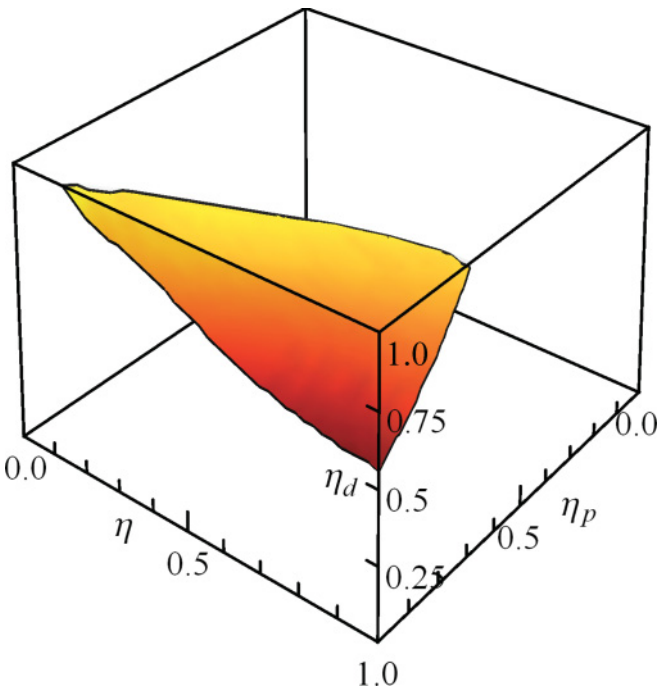

FIG. 3. (Color online) Plot of the feasibility region for beating the standard quantum limit using HB(2) states in the parameter space of preparation inefficiency, interferometer loss, and detector inefficiency η_p, η, and η_d, respectively. The bottleneck in beating the standard quantum limit is the detector imperfection, followed by the preparation imperfection, and, lastly, losses in the interferometer.

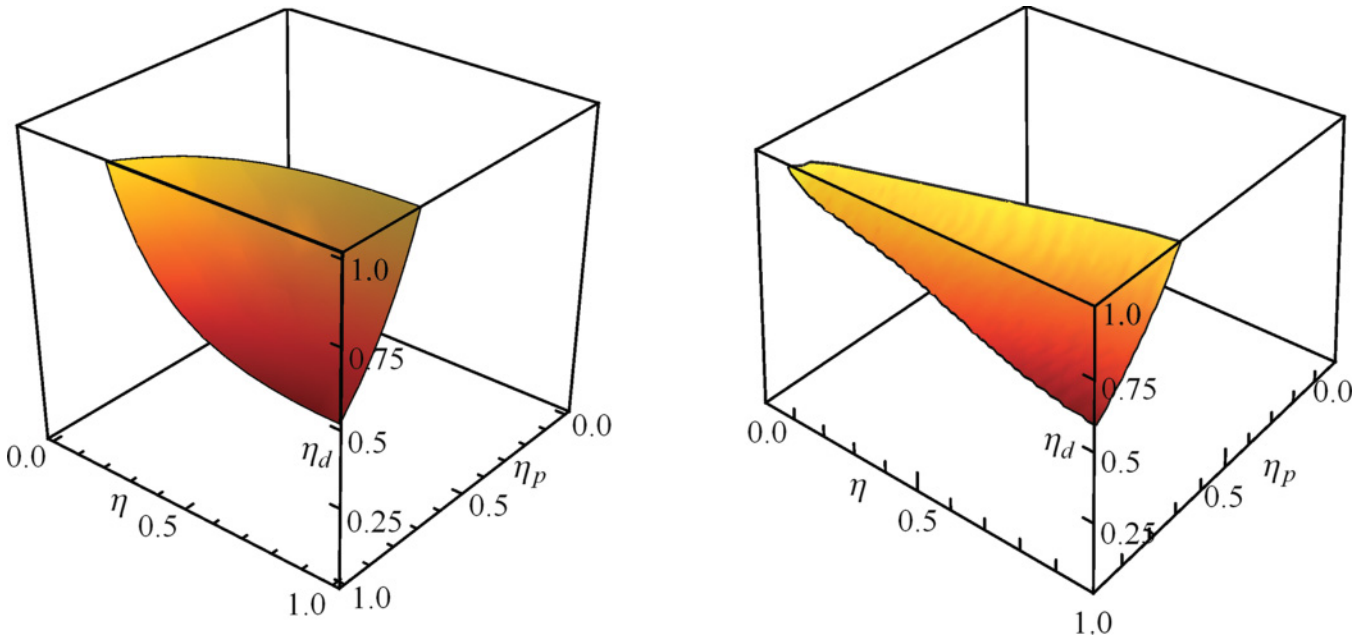

FIG. 4. (Color online) Plot of the feasibility region for beating the standard quantum limit using HB(1) states (left) in the parameter space of preparation inefficiency, interferometer loss, and detector inefficiency η_p, η, and η_d, respectively. The bottleneck in beating the standard quantum limit is the detector imperfection, followed by the preparation imperfection, and, lastly, losses in the interferometer. Same for HB(3) states (right).

on η_p and η_d. Thus, with increasing photon numbers, the feasibility region would shrink along the two axes denoting the imperfections, and extend along that denoting loss, as shown in Fig. 4. It is also easy to see that this particular pattern is universal. The detector and preparation imperfections are identical as far as $F_{(N=k)}$ is concerned, so we can think in terms of only η_p. As discussed previously, the HB state is quite resilient to losses in the interferometer, but to achieve this performance relies on precisely preparing the twin Fock state and performing Fock-state-projection measurements. Thus, η_p and, consequently, η_d have more stringent requirements than η.

To experimentally realize an improvement over its classical counterpart, quantum phase estimation with HB states requires high-quality state preparation and detection in addition to low-loss interferometers. In a realistic experiment with 95% interferometer transmission and 60% detection efficiency (at the high end for commercially available Silicon avalanche photodiodes), the HB(2) state preparation must be better than $\eta_p \geqslant 0.91$, which is well beyond the current state of the art [10]. Using the best PNRDs available, with detection efficiencies approaching 0.98 [20], relaxes the preparation of the HB(2) state to $\eta_p \geqslant 0.71$, which is within the currently attainable values of $0.4 \leqslant \eta_p \leqslant 0.85$ [18].

IV. CONCLUSIONS

We have identified benchmarks for the preparation, detection, and interferometer quality in a practical demonstration of quantum-enhanced metrology. Most importantly, we have shown the first two of these to be the most detrimental to beating the SQL. We have shown that HB states deliver close to the best possible precision in the presence of all these imperfections and losses. Since a scalable route for preparation of the HB states has been proposed [10], we concluded that, if one considers the whole gamut of issues involved in a metrological setup, including state preparation and the final measurement, and uses the objective tool of classical and quantum Fisher information, HB states and PNRDs provide a scalable and practically realizable setup for quantum-enhanced metrology.

ACKNOWLEDGMENTS

This work was funded in part by EPSRC (Grant No. EP/H03031X/1), the European Commission (FP7 Integrated Project Q-ESSENCE, Grant No. 248095, and the EU-Mexico Cooperation Project No. FONCICYT 94142), and the US European Office of Aerospace Research and Development (Grant No. 093020).

APPENDIX A: QUANTUM FISHER INFORMATION OF A LOSSY HB(N) STATE

Since mode e of the state in Eq. (4) of the text is to be traced over, we can rewrite it as

$$|\Psi\rangle = \sum_{m=0}^{2N} |\psi_m\rangle|m\rangle_e, \tag{A1}$$

with

$$|\psi_m\rangle = \frac{1}{2^N} \sum_{k=0}^{N-\lceil \frac{m}{2} \rceil} C_{k+\lceil \frac{m}{2} \rceil} B_{k+\lceil \frac{m}{2} \rceil,m} |2k\rangle_d |2N-2k\rangle_f \tag{A2}$$

for m even. For odd m, replace $2k \to 2k+1$ in the ket. The expressions for B and C are provided in the text. Evaluation of the quantum Fisher information for phase estimation with the lossy states in Eq. (A1) is simplified by their block diagonal

form. Setting $|\tilde{\psi}_m\rangle = |\psi_m\rangle/\sqrt{\mathfrak{N}_m}$, with $\mathfrak{N}_m = \langle\psi_m|\psi_m\rangle$, we get $\mathcal{J} = \sum_{m=0}^{2N} \mathfrak{N}_m \mathcal{J}(|\tilde{\psi}_m\rangle)$. Here, J is given by Eq. (2) in the text and leads to

$$\mathcal{J}(|\tilde{\psi}_m\rangle) = \frac{16}{2^{2N}\mathfrak{N}_m} \sum_{k=0}^{N-\lceil \frac{m}{2} \rceil} \left(k + \left\lceil \frac{m}{2} \right\rceil\right)^2 C^2_{k+\lceil \frac{m}{2} \rceil} B^2_{k+\lceil \frac{m}{2} \rceil, m} \times \left(1 - \frac{C^2_{k+\lceil \frac{m}{2} \rceil} B^2_{k+\lceil \frac{m}{2} \rceil, m}}{\mathfrak{N}_m}\right). \tag{A3}$$

APPENDIX B: CLASSICAL FISHER INFORMATION FOR LOSSY INTERFEROMETER AND IMPERFECT SOURCES AND DETECTORS

Let $U_{ab}(\eta) = e^{i\theta(a^\dagger b + a b^\dagger)}$ denote a beam splitter across modes a,b with transmissivity $\eta = \cos^2\theta$. Then, using the abbreviation

$$X \circ Y \equiv XYX^\dagger, \tag{B1}$$

the state just after BS1 in modes c and d, σ^1_{cd} is

$$\sigma^1_{cd} = U_{ab} \circ (\rho_a \otimes \rho_b), \tag{B2}$$

where $\rho_a = \sum_{n=0}^{N} \binom{N}{n} \eta_p^n (1-\eta_p)^{N-n} |n\rangle\langle n|$. If ϑ_x denotes the vacuum in a mode x, then the state after BS2 is given by

$$\sigma^2_{pq} = \mathrm{Tr}_e\left[U_{fd}\left(\tfrac{1}{2}\right) \circ U_{ce}(\eta) \circ (P_c \otimes \mathbb{I}_{de}) \circ \left(\sigma^1_{cd} \otimes \vartheta_e\right)\right], \tag{B3}$$

where $P_c = e^{i\phi c^\dagger c}$ is the phase accumulation operator and η denotes the interferometer loss. If the vacuum modes associated with the lossy detectors on modes p,q are labeled p',q', then the probabilities at the two PNRDs are now given by

$$p_{mn} = \langle m,n|\mathrm{Tr}_{p'q'}\left\{[[U_{pp'}(\eta_d) \otimes U_{qq'}(\eta_d)] \circ \left(\sigma^2_{pq} \otimes \vartheta_{p'} \otimes \vartheta_{q'}\right)\right\}|m,n\rangle, \tag{B4}$$

where $m,n \geqslant 0$ and $m+n \leqslant 2N$. Additionally, $p_{mn} = p_{nm}$. Thus, there are in general $(N+1)^2$ independent measurement outcomes. The resulting classical Fisher information, expressed as

$$F = \sum_{m,n} \frac{(\partial p_{mn}/\partial\phi)^2}{p_{mn}}, \tag{B5}$$

is, in general, a function of the phase to be estimated ϕ. For $N = 1$, the probabilities of the different outcomes can be arranged in a matrix given by

$$P_1 = \begin{pmatrix} p_{00} & p_{01} & p_{02} \\ p_{10} & p_{11} & 0 \\ p_{20} & 0 & 0 \end{pmatrix}, \tag{B6}$$

where

$$p_{00} = 1 - (1+\eta)\eta_p\eta_d + \frac{1+\eta^2}{2}\eta_p^2\eta_d^2, \tag{B7a}$$

$$p_{01} = \frac{1+\eta}{2}\eta_p\eta_d - \frac{1+\eta^2}{2}\eta_p^2\eta_d^2, \tag{B7b}$$

$$p_{02} = \frac{1+\eta^2-2\eta\cos 2\phi}{8}\eta_p^2\eta_d^2, \tag{B7c}$$

$$p_{11} = \frac{1+\eta^2+2\eta\cos 2\phi}{4}\eta_p^2\eta_d^2. \tag{B7d}$$

The classical Fisher information can easily be calculated using Eq. (B5), resulting in

$$F_{(N=1)} = \frac{8\eta_p^2\eta_d^2\eta^2(1+\eta^2)\sin^2 2\phi}{1+\eta^4-2\eta^2\cos 4\phi}. \tag{B8}$$

This function is maximized at $\phi = \pi/4$, leading to

$$F_{(N=1)} = \frac{8\eta_p^2\eta_d^2\eta^2}{1+\eta^2}. \tag{B9}$$

For $N = 2$, the probabilities for the different measurement outcomes are

$$P_2 = \begin{pmatrix} p_{00} & p_{01} & p_{02} & p_{03} & p_{04} \\ p_{10} & p_{11} & p_{12} & p_{13} & 0 \\ p_{20} & p_{21} & p_{22} & 0 & 0 \\ p_{30} & p_{31} & 0 & 0 & 0 \\ p_{40} & 0 & 0 & 0 & 0 \end{pmatrix}, \tag{B10}$$

where

$$p_{00} = 1 - 2(1+\eta)\eta_p\eta_d + \frac{5+2\eta+5\eta^2}{2}\eta_p^2\eta_d^2 - \frac{3+\eta+\eta^2+3\eta^3}{2}\eta_p^3\eta_d^3 + \frac{3+3\eta^2+2\eta^4}{8}\eta_p^4\eta_d^4, \tag{B11a}$$

$$p_{01} = (1+\eta)\eta_p\eta_d - \frac{5+2\eta+5\eta^2}{2}\eta_p^2\eta_d^2 + \frac{3+\eta+\eta^2+3\eta^3}{4}\eta_p^3\eta_d^3 - \frac{3+3\eta^2+2\eta^4}{4}\eta_p^4\eta_d^4, \tag{B11b}$$

$$p_{02} = \frac{5+(4-6\cos 2\phi)\eta+5\eta^2}{8}\eta_p^2\eta_d^2 - \frac{9+(5-6\cos 2\phi)\eta(1+\eta)+9\eta^3}{8}\eta_p^3\eta_d^3 - \frac{9+10\eta^2+9\eta^4-6\eta(1+\eta^2)\cos 2\phi}{16}\eta_p^4\eta_d^4, \tag{B11c}$$

$$p_{03} = \frac{3(1+\eta)(1+\eta^2-2\eta\cos 2\phi)}{16}\eta_p^3\eta_d^3 - \frac{3(1+\eta^2)(1+\eta^2-2\eta\cos 2\phi)}{16}\eta_p^4\eta_d^4, \tag{B11d}$$

$$p_{04} = \frac{3}{128}(1+\eta)(1+\eta^2-2\eta\cos 2\phi)^2\eta_p^4\eta_d^4, \tag{B11e}$$

$$p_{11} = \frac{5 + 6\cos 2\phi\eta + 5\eta^2}{8}\eta_p^2\eta_d^2 - \frac{9 + (1 + 6\cos 2\phi)\eta(1 + \eta) + 9\eta^3}{8}\eta_p^3\eta_d^3 - \frac{9 + 2\eta^2 + 9\eta^4 + 6\eta(1 + \eta^2)\cos 2\phi}{16}\eta_p^4\eta_d^4, \tag{B11f}$$

$$p_{12} = \frac{9 + \eta + \eta^2 + 9\eta^3 + 6\eta(1 + \eta)\cos 2\phi}{16}\eta_p^3\eta_d^3 + \frac{9 + 2\eta^2 + 9\eta^4 + 6\eta(1 + \eta^2)\cos 2\phi}{16}\eta_p^4\eta_d^4, \tag{B11g}$$

$$p_{13} = \frac{3}{32}(1 + \eta^4 - 2\eta\cos 2\phi)\eta_p^4\eta_d^4, \tag{B11h}$$

$$p_{22} = \frac{1}{64}[9 + 4\eta^2 + 9\eta^4 + 12(\eta + \eta^3)\cos 2\phi + 18\eta^2\cos 4\phi]\eta_p^4\eta_d^4. \tag{B11i}$$

The classical Fisher information $F_{(N=2)}$ can once again be calculated using Eq. (B5). This expression is then used in the plotting of Fig. 3 in the text.

[1] V. Giovannetti, S. Lloyd, and L. Maccone, Science **306**, 1330 (2005).

[2] S. L. Braunstein and C. M. Caves, Phys. Rev. Lett. **72**, 3439 (1994).

[3] H. Lee, P. Kok, and J. Dowling, J. Mod. Opt. **49**, 2325 (2002).

[4] T. Nagata *et al.*, Science **316**, 726 (2007).

[5] I. Afek, O. Ambar, and Y. Silberberg, Science **328**, 879 (2010).

[6] S. Knysh, V. N. Smelyanskiy, and G. A. Durkin, Phys. Rev. A **83**, 021804 (2011).

[7] U. Dorner *et al.*, Phys. Rev. Lett. **102**, 040403 (2009).

[8] T.-W. Lee *et al.*, Phys. Rev. A **80**, 063803 (2009).

[9] M. Kacprowicz *et al.*, Nat. Photonics **4**, 357 (2010).

[10] N. L. Thomas-Peter *et al.*, e-print arXiv:1007.0870.

[11] M. J. Holland and K. Burnett, Phys. Rev. Lett. **71**, 1355 (1993).

[12] J. Dunningham, K. Burnett, and S. M. Barnett, Phys. Rev. Lett. **89**, 150401 (2002); H. Cable and G. A. Durkin, *ibid.* **105**, 013603 (2010); J. Dunningham and K. Burnett, Phys. Rev. A **70**, 033601 (2004); D. Meiser and M. J. Holland, New J. Phys. **11**, 033002 (2009).

[13] P. Kok, H. Lee, and J. P. Dowling, Phys. Rev. A **65**, 052104 (2002); H. F. Hofmann, *ibid.* **70**, 023812 (2004); P. Walther, M. Aspelmeyer, and A. Zeilinger *ibid.* **75**, 012312 (2007); M. W. Mitchell, J. S. Lundeen, and A. M. Steinberg, Nature (London) **429**, 161 (2004); H. S. Eisenberg J. F. Hodelin, G. Khoury, and D. Bouwmeester, Phys. Rev. Lett. **94**, 090502 (2005); H. Cable and J. P. Dowling, *ibid.* **99**, 163604 (2007); S. Barz, G. Cronenberg, A. Zeilinger, and P. Walther, Nat. Photonics **4**, 553 (2010); C. Wagenknecht *et al.*, *ibid.* **4**, 549 (2010).

[14] K. T. Kapale and J. P. Dowling, Phys. Rev. Lett. **99**, 053602 (2007).

[15] K. T. McCusker and P. G. Kwiat, Phys. Rev. Lett. **103**, 163602 (2009).

[16] R. A. Campos, C. C. Gerry, and A. Benmoussa, Phys. Rev. A **68**, 023810 (2003).

[17] F. W. Sun *et al.*, Euro. Phys. Lett. **82**, 24001 (2008).

[18] P. J. Mosley *et al.*, Phys. Rev. Lett. **100**, 133601 (2008); C. Söller *et al.*, Phys. Rev. A **83**, 031806(R) (2011).

[19] K. Banaszek and W. Wódkiewicz, Phys. Rev. Lett. **76**, 4344 (1996).

[20] A. E. Lita, B. Calkins, L. A. Pellouchoud, A. J. Miller, and S. Nam, *Superconducting transition-edge sensors optimized for high-efficiency photon-number resolving detectors*. Presented at the SPIE Symposium on SPIE Defense, Security, and Sensing, Orlando World Center Marriott Resort and Convention Center, Crystal J1 Ballroom, 3 p.m. April 7, 2010.